International Journal of Microwave and Wireless Technologies, 2011, 3(6), 707–715.
doi:10.1017/S1759078711001000

RESEARCH PAPER

Electromagnetic dosimetry for adult and child models within a car: multi-exposure scenarios

LOUIS-RAY HARRIS[1], MAXIM ZHADOBOV[2], NACER CHAHAT[2] AND RONAN SAULEAU[2]

This paper deals with the numerical dosimetry for adult and children models exposed to CW signals of several wireless communication systems (UMTS, WiMax, and Bluetooth) within a partly shielded environment represented by a realistic car model. More than 20 mono- and multi-source exposure scenarios are considered. Computational results demonstrate that, for all considered exposure scenarios, the specific absorption rate (SAR) is at least 40 times (whole-body average) and 10 times (local SAR) lower than the exposure limits fixed by the International Commission on Non-Ionizing Radiation Protection (ICNIRP). The whole-body average SAR values for children are found to be typically 1.1–1.3 times higher than those of adults. Under several exposure scenarios, the local SAR in the limbs of children models is 2–3 times higher than corresponding values in adult models. The power density distributions within the car have been also analyzed for one, two, and three simultaneously emitting devices. The results show that the homogeneity of the power density distribution increases with increasing number of simultaneously operating transmitters. These data suggest that the use of several wireless communication devices within a car leads to exposure levels that are several orders of magnitude below international exposure limits, even for the multi-exposure scenarios for both adult and children models.

Keywords: Electromagnetic dosimetry, Finite-difference time-domain (FDTD) method, Multi-exposure, Children human body models, Partly shielded environment, Specific absorption rate (SAR)

Received 8 July 2011; Revised 20 October 2011

I. INTRODUCTION

The increasing usage of wireless devices requires rigorous exposure dosimetry studies, particularly for multi-exposure scenarios involving new exposure sources (UMTS, WiMax, etc.). In this context, exposures within vehicular and other types of partly shielded environments are of particular interest.

Recently, several studies have been conducted to investigate the specific absorption rate (SAR) induced by wireless transmitters located inside a vehicle [1–6] and other partly shielded or reverberating environments [7–10]. The effect of varying the orientation of an antenna has been analyzed [1, 11, 12]. It was shown that the presence of a car frame significantly modifies the SAR induced in a cell phone user [1, 6].

In most of the previous works, the SAR and electromagnetic field distributions have been computed for mono-source exposure scenarios (single operating frequency) (e.g. [1]), demonstrating that both local and whole-body average SAR levels vary widely with the number/location of humans and orientation of antennas. In parallel, it has been shown that in-vehicle dielectric structures have a limited impact on the average power density level within a car, whereas they can perturb the local electromagnetic field distribution [13]. Furthermore, it was demonstrated that the window glazing can significantly modify the average power density within a car, particularly for frequencies above 1 GHz [13]. Field coupling with realistic full-size vehicles and simplified vehicle-like structures has also been experimentally assessed [14, 15].

Adult and child human models have been used to assess the SAR induced by mobile phone radiation [16–19]. It is interesting to note that the power absorption in children is significantly different from that in adults due to the morphological differences and variation of dielectric properties primarily related to the reduction of the water content in human tissues with age [20]. It was reported that, depending on the exposure scenario and inter-individual morphological peculiarities, the SAR may be higher in children than in adults [21–23], while other studies showed similar SAR levels [20, 24–26].

In contrast to most of the previously reported results, we focus our attention on exposures induced by new wireless communication devices, with an emphasis on multi-source scenarios. The main purpose of this study is to compute and analyze in detail the whole-body average and local SAR induced in adult and children passengers, as well as the power density distribution within a car model. The exposure parameters and scenarios (new and emerging wireless technologies, exposure of children, and multi-source exposure) correspond to research priorities identified in the Research Agenda of the World Health Organization in 2010 [27].

[1]University of Technology, Kingston, Jamaica.
[2]Institute of Electronics and Telecommunications of Rennes (IETR), UMR CNRS 6164, University of Rennes 1, Rennes, France.
Corresponding author:
Dr. M. Zhadobov
Email: maxim.zhadobov@univ-rennes1.fr

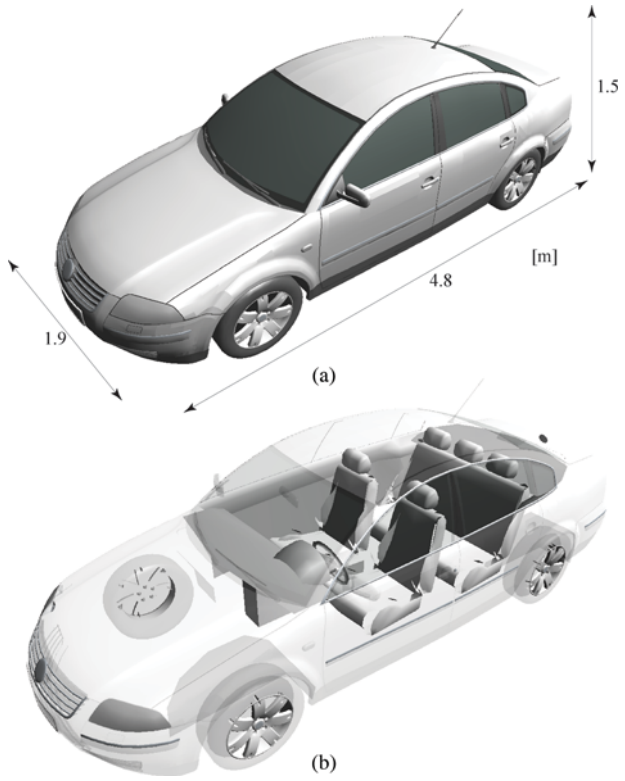

Fig. 1. Car model: (a) External view and dimensions. (b) Internal view and individual parts.

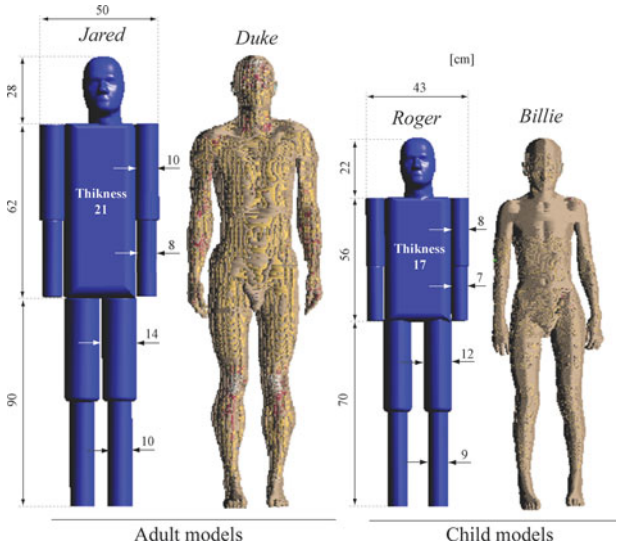

Fig. 2. Homogeneous (Jared/Roger) and voxel (Duke/Billie) body models.

II. MATERIALS AND METHODS

A) Car model

The car model used in simulations is a real-sized VW Passat CAD model imported in *.3ds format (Fig. 1(a)). It has a metallic shell with realistic interior fittings (Fig. 1(b)). Some simplifications have been made compared to the real car. In particular, some small parts, the rear window heater, and metallic frames of the seats are not included in the model. This allows a reduction of the overall mesh size for the computations and does not change the results and conclusions of this study.

The car body, along with the undercarriage, wheels, and other common materials, are set as perfect electric conductors. The dielectric properties of non-metallic materials of the car, including seats and plastic components, are chosen based on values provided in the literature [13]. The permittivity of glass for windows is taken from the SEMCAD X (SPEAG, Zurich, Switzerland) material database. The relative permittivity ε_r used in the simulations are 2.46, 4.82, and 1.14 for plastic, glass, and foam, respectively (used for seats, headrests, and the door lining). The electrical conductivity σ equals 2.9×10^{-3}, 4.3×10^{-3}, and 2×10^{-4} S/m, respectively.

B) Human models

To control the positioning of the body in a flexible way, we have designed a homogenous adult phantom, called Jared, based on dimensions of the non-homogenous voxel Virtual Family's Duke phantom provided by SPEAG [28] (Fig. 2). Its height and average dimensions of the body parts are equal to those of the Duke model. Additionally, the specific anthropomorphic mannequin (SAM) phantom head has been incorporated into the design. In a similar way, a homogenous numerical child phantom (Roger) has been designed based on the Virtual Family's Billie voxel model.

The dielectric properties of the Jared and Roger models are assigned as 2/3 equivalent muscle model at 2.3GHz ($\varepsilon_r = 35.3$ and $\sigma = 1.1$ S/m) [29]. Here, the dispersion of dielectric properties is neglected in the 2.1–2.5 GHz band as the relative variations of the complex permittivity in this frequency range are below 1%. While a generally accepted set of values for the dielectric constant and conductivity for child models has not yet been developed, some studies have demonstrated that the variation of dielectric properties in children does not result in significant changes of the SAR [20, 26].

To assess the differences between the homogeneous and non-homogeneous models, three exposure situations have been considered: (1) generic monopole [30] located close to the left hip; (2) generic monopole close to the head; and (3) plane wave illumination. We considered the standing position and a random non-standing position. The computational results demonstrated that, in identical positions, the differences in the local 10 g-averaged SAR between Duke and Jared and between Roger and Billie models range from 10 to 15% (in most of the cases, the SAR was higher for homogeneous models). For all exposure scenarios, the difference in terms of the whole-body average SAR is less than 10%. Furthermore, for the generic monopole, the maximal difference in S_{11} does not exceed 1–2 dB depending on the exposure scenario, and the computed radiation patterns are almost identical. This proves the appropriateness of the considered homogeneous models.

C) Transmitting devices and positioning

The car layout with human models and transmitting devices is shown in Fig. 3. We consider here UMTS, WiMax, and Bluetooth transmitters operating at 2.1GHz (allocated for Europe), 2.5 and 2.45 GHz, respectively. All signals are assumed to be narrowband and non-modulated. The transmitting devices are further denoted as DR (driver) UMTS,

https://doi.org/10.1017/S1759078711001000 Published online by Cambridge University Press

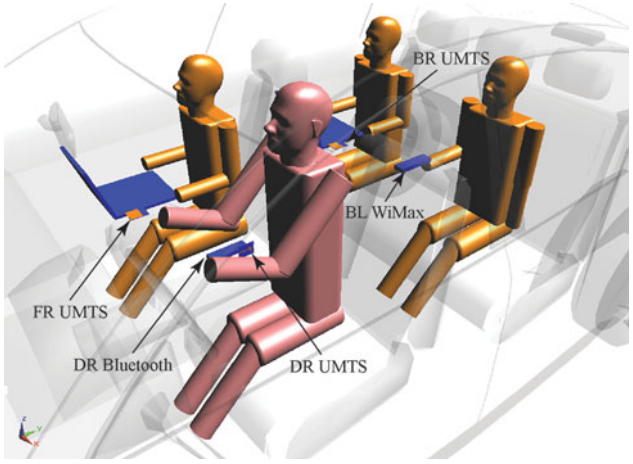

Fig. 3. CAD model of an adult driver (DR), three child passengers, and wireless devices inside the car. Note that both DR devices are positioned close to the right DR hip on the panel separating the DR and FR (front-right) passengers.

FR (front-right) UMTS, BR (back-right) UMTS, BL (back-left) WiMax, and DR Bluetooth.

An inverted F-type antenna with substrate dimensions of $50 \times 60 \times 1.6\ \text{mm}^3$ is used as the UMTS transmitter (Fig. 4(a)) [30]. A generic monopole is used as the WiMax and Bluetooth transmitter (Fig. 4(b)) [30]. The length of the monopole (30 mm) was chosen to match the antenna at 2.45–2.5 GHz. For both devices, the S_{11} characteristics in free space and in the center of the car show similar behavior (Fig. 4).

The maximum radiated power of a UMTS device ranges from 125 to 250 mW. It equals about 200 mW for a WiMax device, whereas for the Bluetooth, it is around 2 mW. Under normal operating conditions, the radiated power is below the peak value. However, in our simulations, we use the peak values that correspond to worst-case scenarios.

D) Numerical modeling

The full-wave finite-difference time-domain (FDTD) electromagnetic solver SEMCAD X (SPEAG, Zurich, Switzerland)

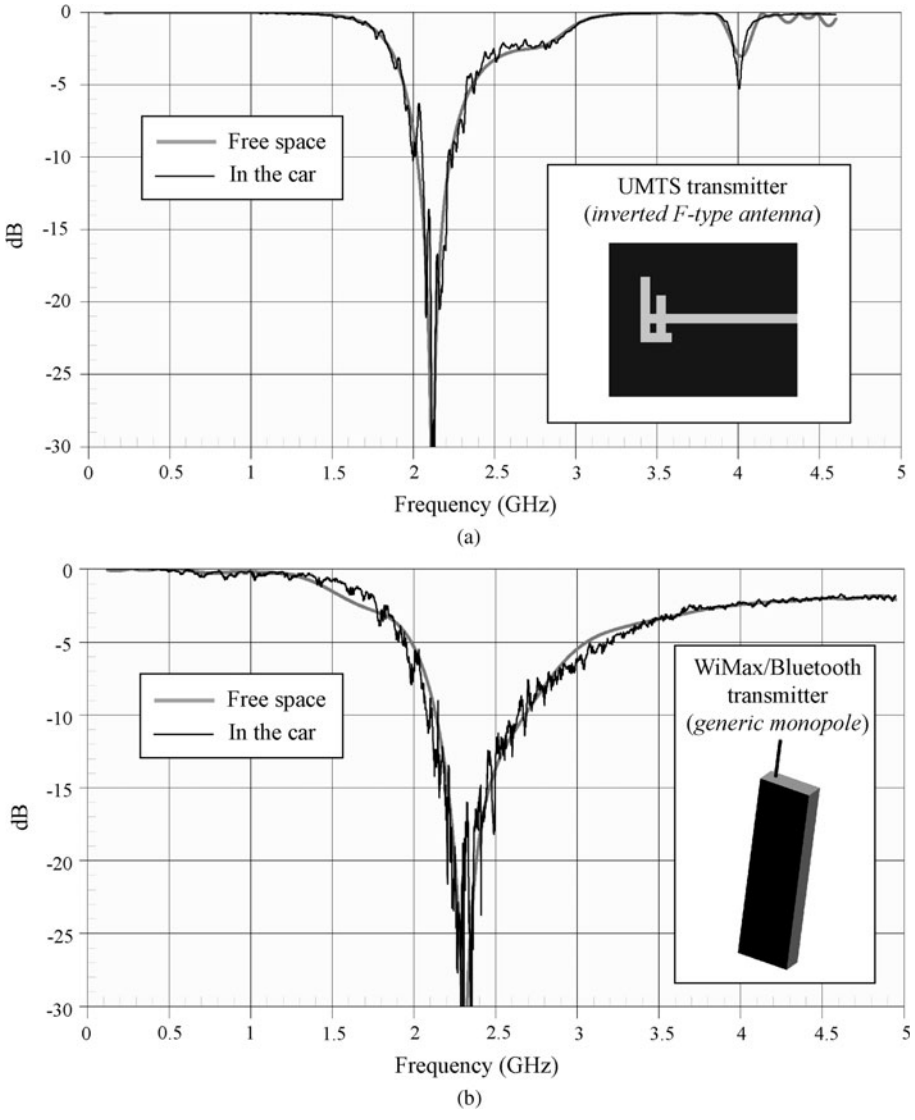

Fig. 4. Return loss of transmitting devices in free space and in the car: (a) UMTS. (b) WiMax and Bluetooth.

https://doi.org/10.1017/S1759078711001000 Published online by Cambridge University Press

has been used to perform simulations. The accuracy of this technique has already been validated in many computational dosimetry studies [31].

The data are obtained for a computational domain that includes the entire real-size car model. This results in increased RAM requirements (typically 15–20 Gb) and computational time (around 24 h with two 2.3 GHz four-core CPU) compared to scaled-down models, but is important for providing an acceptable computational accuracy. Perfectly Matched Layer (PML) boundary conditions have been used to simulate the anechoic environment. The boundaries are placed at least 20 mesh cells from the structure. The simulations convergence is systematically checked inside the car, and also at the furthest points from the antenna (corners of the computational volume). Approximately 200 periods are required to reach convergence.

Preliminary computations have been carried out to determine a suitable mesh resolution for the problem space before adding the human models. It has been found that numerical results remain the same in terms of S_{11} of antennas and power density distribution for mesh spacing below 15 mm. For the human models, any mesh cell size less than 5 mm inside the body does not significantly alter SAR results. A similar mesh resolution was also used in [11, 12]. In the region of the transmitters, as well as in some problem regions (curvatures, small important sub-structures and details, high electromagnetic field, etc.), a non-uniform meshing (down to 0.3 mm) with cell-to-cell gradients of 1.2–1.3 is applied. These relatively small gradients allow minimizing numerical dispersion. In simulations, each body model is represented by over 10 million mesh cells, and the total computational volume is about 150 million mesh cells.

III. NUMERICAL RESULTS

We present here the computational results for the whole-body average and local SAR (main dosimetric quantity below 10 GHz) for different multi-exposure scenarios. Then the power density distributions are analyzed. Two situations have been studied and compared: (1) four adult models in the car; (2) one adult (DR), and three children models (Fig. 3).

A) Whole-body average SAR

Table 1 indicates the whole-body average SAR for one transmitting device inside the vehicle. As expected, the highest SAR values are observed for the humans closest to the transmitting device, and the SAR decreases with increasing distance from the transmitter. The highest values (1.39 mW/kg for adults and 1.58 mW/kg for DR and children) are found for the

Table 1. Mean SAR values for single-user scenarios.

	Whole-body average SAR (mW/kg)			
	DR UMTS	**FR UMTS**	**BR UMTS**	**BL WiMax**
DR	**1.39/1.58***	0.65/0.55	0.33/0.30	0.03/0.008
FR	0.43/0.60	**0.95/1.00**	0.17/0.18	0.03/0.003
BR	0.12/0.21	0.03/0.03	**0.86/1.07**	0.15/0.066
BL	0.20/0.34	0.08/0.09	0.39/0.44	**0.89/1.28**

*Four adults/DR and three children.

Table 2. Power absorbed in the body for single-user scenarios.

	Power absorbed in the body (mW)			
	DR UMTS	**FR UMTS**	**BR UMTS**	**BL WiMax**
DR	**36.9***/—	17.3/14.6	8.7/7.9	0.8/0.2
FR	11.4/12.1	**24.9/20.1**	4.5/3.6	0.7/0.06
BR	3.3/4.3	0.8/0.5	**22.9/21.6**	4.1/1.3
BL	5.4/6.9	2/1.7	10.4/8.9	**23.9/25.8**

*Four adults/DR and three children.

Table 3. Mean SAR values for scenarios with DR and passenger transmitting devices.

	Whole-body average SAR (mW/kg)		
	DR UMTS + FR UMTS	**DR UMTS + BR UMTS**	**DR UMTS + BL WiMax**
DR	**2.04/2.13***	**1.72/1.88**	**1.42/1.60**
FR	**1.38/1.60**	0.60/0.78	0.46/0.60
BR	0.15/0.24	**0.98/1.28**	0.28/0.28
BL	0.28/0.43	0.59/0.77	**1.09/1.60**

*Four adults/DR and three children.

Table 4. Power absorbed in the body for scenarios with DR and passenger transmitting devices.

	Power absorbed in the body SAR (mW)		
	DR UMTS + FR UMTS	**DR UMTS + BR UMTS**	**DR UMTS + BL WiMax**
DR	**54.2***/—	**45.6**/—	**37.7**/—
FR	**36.3/32.2**	15.9/15.7	12.3/12.2
BR	4.1/4.8	**26.2/25.9**	7.4/5.6
BL	7.4/8.6	15.8/15.8	**29.3/32.7**

*Four adults/DR and three children.

Table 5. Mean SAR values for other two-user scenarios.

	Whole-body average SAR (mW/kg)		
	FR UMTS + BR UMTS	**FR UMTS + BL WiMax**	**BR UMTS + BL WiMax**
DR	0.98/0.85*	0.68/0.56	0.36/0.31
FR	**1.12/1.17**	**0.98/1.00**	0.20/0.18
BR	**0.89/1.10**	0.19/0.069	**1.01/1.14**
BL	0.47/0.52	**0.97/1.36**	**1.28/1.72**

*Four adults/DR and three children.

Table 6. Mean SAR values for a Bluetooth device.

Whole-body average SAR (mW/kg) DR Bluetooth	
DR	0.0036/0.0015*
FR	0.0062/0.0045
BR	0.00080/0.00061
BL	0.00055/0.00044

*Four adults/DR and three children.

https://doi.org/10.1017/S1759078711001000 Published online by Cambridge University Press

Table 7. Localized SAR for scenarios with DR UMTS or FR UMTS.

	Localized SAR (mW/kg)			
	DR UMTS		FR UMTS	
	Head/Trunk	Limbs	Head/Trunk	Limbs
DR	**20.2/25.3***	**23.4/24.1**	6.5/5.4	11.5/13.5
FR	5.6/8.8	14.6/14.8	**11.2/7.2**	**54.7/170.6**
BR	0.7/0.9	6.4/4.4	0.2/0.13	0.8/0.51
BL	0.93/1.9	6.8/10.5	0.6/0.4	2.2/1.6

*Four adults/DR and three children.

Table 8. Localized SAR values for scenarios with BR UMTS or BL WiMax.

	Localized SAR (mW/kg)			
	BR UMTS		BL WiMax	
	Head/Trunk	Limbs	Head/Trunk	Limbs
DR	3.5/1.9*	2.9/2.9	0.56/0.2	0.53/0.2
FR	4.0/2.5	1.9/1.8	0.7/0.06	0.9/0.17
BR	**15.9/4.6**	**80.5/187.4**	4.1/0.6	4.6/4.4
BL	2.9/3.2	10.3/14.9	**8.7/7.2**	**302.2/392.6**

*Four adults/DR and three children.

operating UMTS device positioned between the DR and FR passenger. For the same transmitter, the next highest value is observed for the FR passenger, and it is decreased by a factor of 3.2 (adults)/2.6 (children) compared to the maximum SAR in the DR model. As expected, the SAR induced in the rear passengers is much lower since the distance from the transmitter is greater. Similar trends are found for other transmitting devices. The results also demonstrate that the whole-body average SAR values for the scenario "DR + children" are typically 1.1–1.3 times higher than those of adults. In most of the scenarios, the power absorbed by the body is higher for the adult models due to the increased weight and body surface (Table 2). However, some of the exposure scenarios demonstrate the opposite (e.g. DR UMTS).

Table 3 shows average SAR values resulting from the combination of the DR device and one other device transmitting simultaneously. For these scenarios, the total absorbed power is also provided in Table 4. In all cases, the maximum mean SAR is detected for the DR. It is interesting to note that the DR is strongly exposed even when FR UMTS and BR UMTS are operating (Table 5). We restricted our consideration to two radiating devices as a higher number of transmitters simultaneously operating at the peak power are not realistic.

In all the scenarios considered above, the SAR values are roughly 40–2000 times below the ICNIRP whole-body average SAR general public exposure limit of 80mW/kg [32]. Moreover, the data provided in Table 6 indicate that exposure levels induced by a Bluetooth transmitting device are even lower (over 10^5 times less) mainly because of the very low radiating power (2 mW). Further, we eliminate Bluetooth from the consideration as its contribution to the total SAR is expected to be negligible.

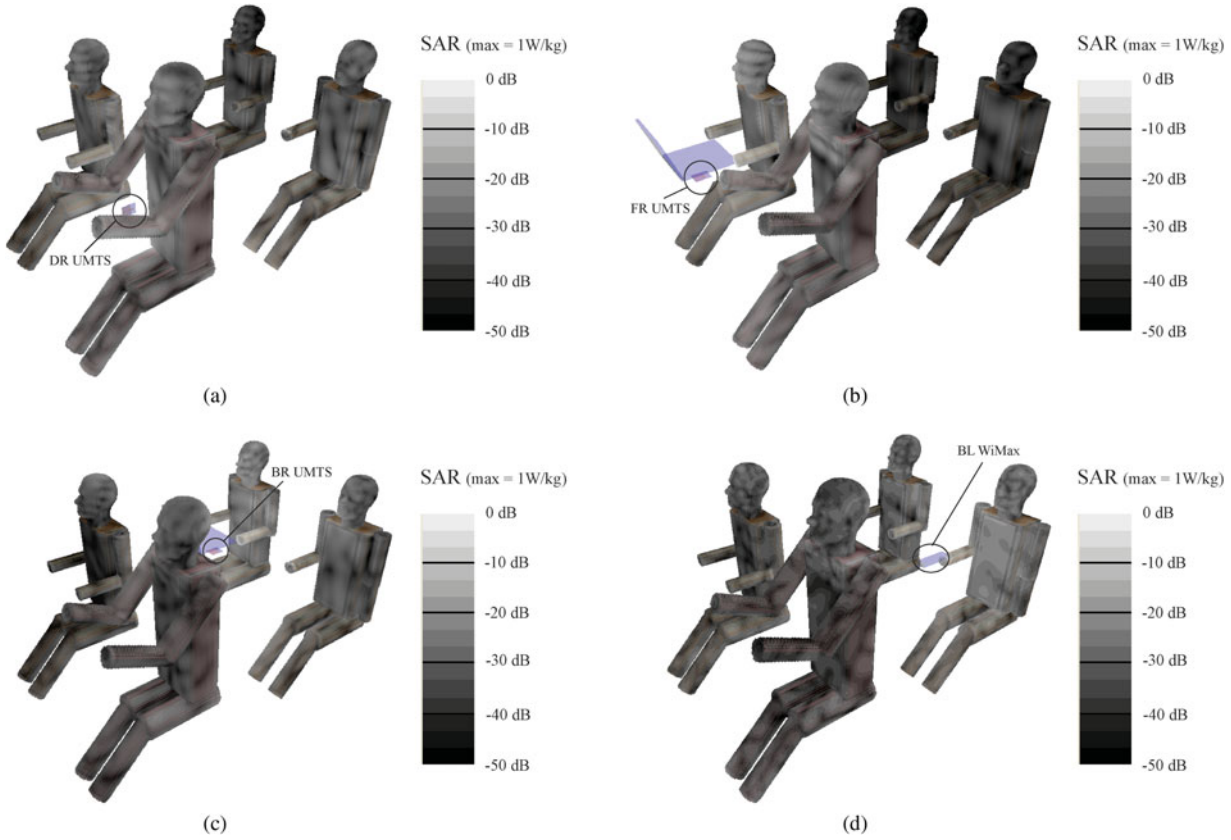

Fig. 5. Surface SAR distribution for various operating transmitters (DR and three children models within the car). (a) DR UMTS. (b) FR UMTS. (c) BR UMTS. (d) BL WiMax.

https://doi.org/10.1017/S1759078711001000 Published online by Cambridge University Press

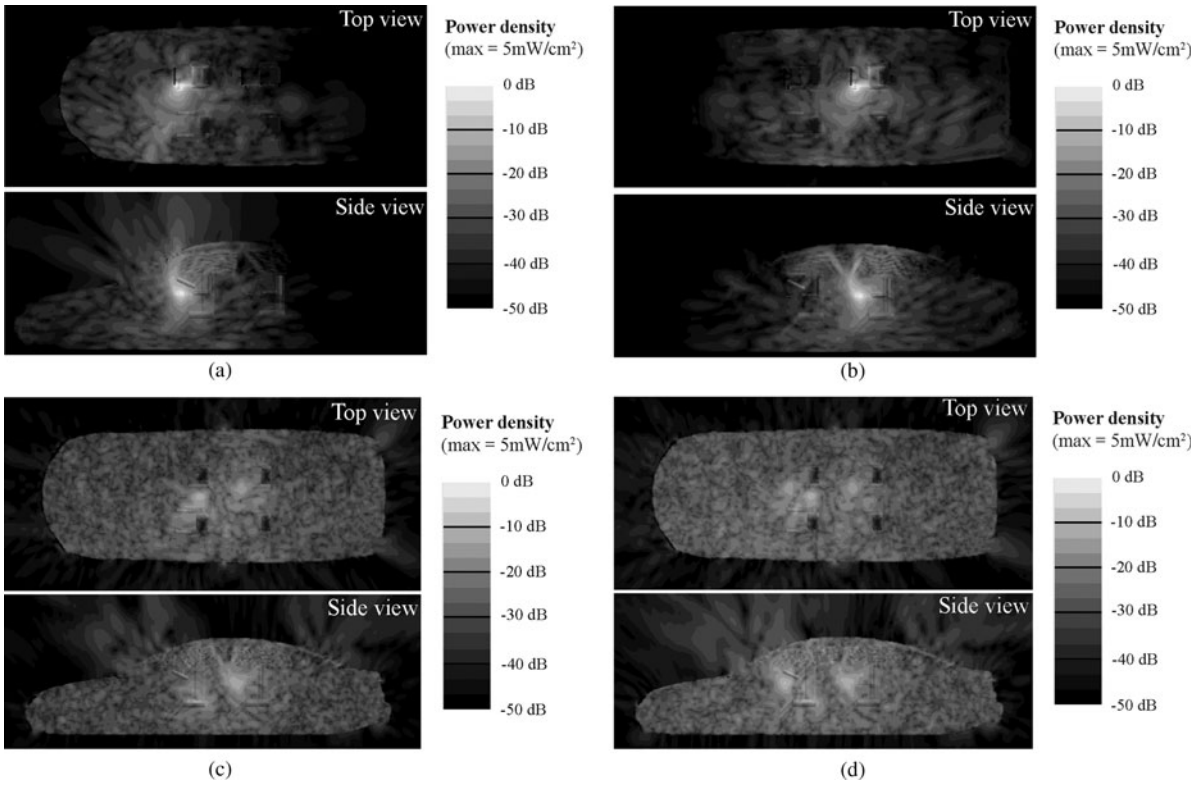

Fig. 6. Power density distribution within the car for mono-source (a, b) and multi-source exposures (c, d). (a) FR UMTS. (b) BR UMTS. (c) DR UMTS and BR UMTS. (d) DR UMTS, FR UMTS, and BR UMTS.

B) Local SAR

The maximum 10 g-averaged localized SAR in the head, trunk, and limbs are presented in Tables 7 and 8. For four adult passengers, the values for the head and trunk range from roughly 10^2 to over 10^4 times less than the limit of 2 W/kg set by the ICNIRP for the localized SAR [32]. For the limbs, the maximum SAR values are $13–2 \times 10^4$ times less than the ICNIRP limit of 4 W/kg.

However, when the child models are used, for several scenarios (e.g. FR UMTS and BL UMTS), the localized SAR in the limbs of users is 2–3 times higher than the corresponding values in adult models. The maximal local SAR (393 mW/kg) is observed in a child passenger model for the BL WiMax scenario (Table 8); this maximal value is roughly 10 times below the ICNIRP limit.

The surface SAR distribution for the exposure scenarios considered in Tables 7 and 8 for children passengers are shown in Fig. 5. It is worthwhile to note that, at the considered frequencies, the peak SAR is expected at the body surface due to the relatively superficial absorption in the tissues (the penetration depth in the body is of the order of 1cm).

C) Power density distributions within the car

The power density distributions within the car in horizontal and vertical slices are presented in Fig. 6. The results are shown for two mono-source and two multi-source exposure scenarios for a configuration with DR and three children passengers.

For the mono-source scenarios, two cut planes pass through the transmitting device. For the front-positioned devices (Fig. 6(a)), the power density is mainly concentrated in the front part of the car, and the signal levels at the rear passengers' position are below 0.05mW/cm². A significant part of the power is transmitted through the front window (power density up to 1 mW/cm²). The highest total SAR absorbed by the DR and passengers corresponds to the DR UMTS exposure as in this scenario none of the passengers are shadowed by one another.

For a rear-positioned transmitting device (Fig. 6(b)), most of the power is localized in the center of the car due to the reflections from the roof and bottom of the car and significant absorption in the DR, passengers, and car seats. These results are consistent with the whole-body averaged SAR data provided in Table 1.

For the multi-source scenarios, the vertical and horizontal cut planes pass between the emitting devices. Figs 6(c) and 6(d) show exposure scenarios where two and three sources radiate simultaneously. Two phenomena are observed with the increasing number of transmitting devices: (1) homogenization of the power density distribution within the car; and (2) increase of the average power density.

IV. DISCUSSION AND CONCLUSION

A detailed electromagnetic dosimetry study has been performed to numerically quantify the SAR and power density distributions of several wireless communication devices within a realistic car model. Mono- and multi-source scenarios have been investigated and compared to provide an insight into the multi-exposure phenomena that may occur within partly shielded environments. The results obtained for the adult models are compared with those obtained for the children models.

https://doi.org/10.1017/S1759078711001000 Published online by Cambridge University Press

First, the whole-body average SAR and total power absorbed in the body have been computed for single or two simultaneously transmitting devices inside the vehicle. For a single operating device, the maximum SAR for adults and for DR and children exposure is 1.39 and 1.58 mW/kg, respectively. For two simultaneously emitting sources, these values increase to 2.04 and 2.13 mW/kg. For all considered exposure scenarios, the whole-body average SAR is more than 40 times lower than the ICNIRP general public exposure limit.

Second, we assessed the maximum 10 g-averaged localized SAR in the head, trunk, and limbs. The maximum SAR values are found in the limbs, and they are at least 10 times lower than ICNIRP limits for both adult and children models. As the maximal local SAR is expected to appear in the near-surface region of the body at considered frequencies, we also computed the surface SAR distribution for the DR and children models.

Third, the power density distributions within the car have been analyzed for one, two, and three simultaneously emitting devices. It is demonstrated that the uniformity of the power density distribution increases with an increasing number of simultaneously operating transmitters.

Finally, it is interesting to note that, because of the smaller surface and volume of the body, the whole-body average SAR values for children are typically 1.1–1.3 times higher than those of adults. However, under some exposure scenarios, localized SAR in the limbs of child users is 2–3 times higher than the corresponding values in adult models.

In this study, we restricted our consideration to the numerical analysis mainly because of two reasons: (1) the FDTD technique implemented in the SEMCAD X simulator has already been validated in many dosimetry studies; and (2) experimental confirmation of the obtained results is an extremely challenging task, taking into account the determination of the exposure levels inside the human body in a sitting position and utilization of vehicles, and it might be the subject of a separate investigation.

In conclusion, this study has demonstrated that the use of UMTS, WiMax, and Bluetooth devices within a car leads to exposure levels that are several orders of magnitude below the international exposure limits, even for the worst-case multi-exposure scenarios. These results suggest that these devices can be safely used within a car as they are in compliance with the international exposure limits.

ACKNOWLEDGEMENTS

This work was supported by "Agence Nationale de la Recherche" (ANR), France, under Grant ANR-09-RPDOC-003-01 (Bio-CEM project), by University of Rennes 1, France, under Grant 991R691M, and by "Centre National de la Recherche Scientifique (CNRS)", France. The authors thank Peter Futter from SPEAG for his kind support related to the numerical modeling using SEMCAD.

REFERENCES

[1] Anzaldi, G.; Silva, F.; Fernandez, M.; Quilez, M.; Riu, P.: Initial analysis of SAR from a cell phone inside a vehicle by numerical computation. IEEE Trans. Biomed. Eng., **54** (2007), 921–930.

[2] Ruddle, A.R.: Efficient estimation of human field exposure threats for vehicles with internal transmitters at microwave frequencies, in Proc. 16th ITS World Congress, Stockholm, Sweden, September 21–25, 2009.

[3] Zhang, H.; Low, L.; Rigelsford, J.; Langley, R.: Electromagnetic field mitigation within a cavity with vehicle-like features, in Proc. Fourth European Conf. Antenna Propagation, Barcelona, Spain, April 12–16, 2010.

[4] Low, L.; Zhang, H.; Rigelsford, J.; Langley, R.: Measured and computed in-vehicle field distributions, in Proc. Fourth European Conf. Antenna Propagation, Barcelona, Spain, April 12–16, 2010.

[5] Ruddle, A.; Low, L.; Zhang, H.; Rigelsford, J.; Langley, R.: Computed SAR and field exposure threat assessment for vehicle occupants, in Proc. Fourth European Conf. Antenna Propagation, Barcelona, Spain, Apr. 12–16, 2010.

[6] Chan, K.H.; Leung, S.W.; Siu, Y.M.: Specific absorption rate evaluation for people using wireless communication device in vehicle, in Proc. IEEE Int. Symp. Electromagnetic Compatibility (EMC), Fort Lauderdale, FL, USA, July 25–30, 2010, 706–711.

[7] Simba, A.Y.; Hikage, T.; Watanabe, S.; Nojima, T.: Specific absorption rates of anatomically realistic human models exposed to RF electromagnetic fields from mobile phones used in elevators. IEEE Trans. Microwave Theory Tech., **57** (2009), 1250–1259.

[8] Tropainen, A.: Human exposure by mobile phones in enclosed areas. Bioelectromagnetics, **24** (2003), 63–65.

[9] Ferrer, J.; Fernandez-Seivane, L.; Hernando, J.M.; Castan, M.B.; Garcia, L.; Vazquez, J.M.: On the exposure to mobile phone radiation in trains. Appl. Phys. Lett., **86** (2005), 224101.

[10] Tang, C.K.; Chan, K.H.; Fung, L.C.; Leung, S.W.: Effect on radiofrequency human exposure of mobile phone inside an enclosed metallic elevator. Microwave Opt. Tech. Lett., **50** (2008), 2207–2210.

[11] Ruddle, A.: Computed SAR levels in vehicle occupants due to on-board transmissions at 900 MHz, in Proc. Loughborough Antennas and Propagation Conf., Loughborough, UK, November 16–17, 2009, 137–140.

[12] Ruddle, A.: Simulation of in-vehicle SAR levels at 900 MHz for a car with various transmitter positions and human occupancy configurations, in Proc. 31st Annual Meeting of the BEMS, Davos, Switzerland, June 15–19, 2009.

[13] Ruddle, A.: Influence of dielectric materials on in-vehicle electromagnetic fields, in Proc. IET Seminar on Electromagnetic Propagation in Structures and Buildings, London, UK, December 2008.

[14] Ruddle, A.R.; Ferrières, X.; Parmantier, J.P.; Ward, D.D.: Experimental validation of time-domain electromagnetic models for field coupling into the interior of a vehicle due to a nearby broadband antenna. IEE Proc. Sci. Meas. Technol., **151** (6) (2004), 430–433.

[15] Horiuchi, S.; Yamada, K.; Tanaka, S.; Yamada, Y.; Michishita, N.: Comparisons of simulated and measured electric field distributions in a cabin of a simplified scale car model. IEICE Trans. Commun., **90** (2007), 2408–2415.

[16] Gandhi, O.P.; Lazzi, G.; Furse, C.: Electromagnetic absorption in the human head and neck for mobile telephones at 835 and 1900 MHz. IEEE Trans. Microw. Theory Tech., **44** (1996), 1884–1897.

[17] De Salles, A.A.; Bulla, G.; Rodriguez, C.E.: Electromagnetic absorption in the head of adults and children due to mobile phone operation close to the head. Electromagn. Biol. Med., **25** (2006), 349–360.

[18] Schoenborn, F.; Burhardt, V.; Kuster, N.: Difference in energy absorption between heads of adults and children in the near field of sources. Health Phys., **74** (1998), 160–168.

[19] Wang, J.; Fujiwara, O.: Comparison and evaluation of electromagnetic absorption characteristics in realistic children for 900-MHz

mobile telephones. IEEE Trans. Microw. Theory Tech., **51** (2003), 966–971.

[20] Peyman, A.; Gabriel, C.; Grant, E.H.; Vermeeren, G.; Martens, L.: Variation of the dielectric properties of tissues with age: the effect on the values of SAR in children when exposed to walkie-talkie devices. Phys. Med. Biol., **54** (2009), 227–241.

[21] Hadjem, A.; Lautru, D.; Dale, C.; Wong, M.F.; Hanna, V.F.; Wiart, J.: Study of specific absorption rate (SAR) induced in the two child head models and adult heads using mobile phones. IEEE Trans. Microw. Theory Tech., **53** (2005), 4–11.

[22] Wiart, J. et al.: Modeling of RF head exposure in children. Bioelectromagnetics, **S7** (2005), 19–30.

[23] Wiart, J.; Hadjem, A.; Wong, M.F.; Bloch, I.: Analysis of RF exposure in the head tissues of children and adults. Phys. Med. Biol., **53** (2008), 3681–3695.

[24] Beard, B.B. et al.: Comparisons of computed mobile phone induced SAR in the SAM phantom to that in anatomically correct models of the human head. IEEE Trans. Electromagn. Compat., **48** (2006), 397–407.

[25] Keshvari, J.; Keshvari, R.; Lang, S.: The effect of increase in dielectric values on specific absorption rate (SAR) in eye and head tissues following 900, 1800 and 2450 MHz radio frequency (RF) exposure. Phys. Med. Biol., **51** (2006), 1463–1477.

[26] Christ, A. et al.: Age dependent changes in SAR and temperature distribution induced in the user's head by cellular phones, in Proc. 30th Annual Meeting of BEMS, San Diego, CA, USA, June 8–12, 2008, 131.

[27] World Health Organization.: "Research agenda for radiofrequency fields," 2010. [Online]. www.who.int/peh-emf/research/agenda.

[28] Online at http://www.itis.ethz.ch/index/index_humanmodels.html

[29] 1528–2003, IEEE Recommended Practice for Determining the Peak Spatial-Average Specific Absorption Rate (SAR) in the Human Head From Wireless Communications Devices: Measurement Techniques, 2003.

[30] Schmid & Partner Engineering AG, SEMCAD X Tutorial, February 2010.

[31] Online at http://www.speag.com/products/semcad/publications-reviews/cover-articles-books.

[32] ICNIRP.: Guidelines for limiting exposure to time-varying electric, magnetic, and electromagnetic fields (up to 300 GHz). Health Phys., **74** (1998), 494–522.

Louis-Ray Harris received the B.Sc. in Electrical and Computer Engineering from the University of the West Indies, Trinidad, in 1999. He subsequently received the M.Sc. in Space Communications Engineering from the Lancaster University, England, in 2001. In 2004, he received the Monbukogakusho Scholarship (Japan), where his research involved work in the area of radio propagation estimation methods. He received his Ph.D. degree in Wireless Communications from the Hokkaido University, Japan. His research interests include investigating the application of the finite-difference time-domain (FDTD) analysis method to various scenarios involving indoor WLANs. In 2009, he joined the Institute of Electronics and Telecommunications of Rennes (IETR), France, where he carried out post-doctoral research which focused on body-centric communications and the modeling of wireless devices in vehicular environments. He is currently a member of the faculty of the School of Engineering at the University of Technology, Jamaica.

Maxim Zhadobov received the M.S. degree in radiophysics from Nizhni Novgorod State University, Russia, in 2003, and the Ph.D. degree in bioelectromagnetics from Institute of Electronics and Telecommunications of Rennes (IETR), France, in 2006. He accomplished post-doctoral training at the Center for Biomedical Physics, Temple University, Philadelphia, USA, in 2008 and then rejoined IETR as an Associate Researcher CNRS. His main scientific interests are in the field of biocompatibility of electromagnetic radiations, including interactions of microwaves, millimeter waves and pulsed radiations at the cellular and sub-cellular levels, optimization of body-centric wireless systems, experimental and numerical electromagnetic dosimetry, health risks and environmental safety of emerging wireless communication systems, biocompatibility of wireless biomedical techniques, and therapeutic applications of non-ionizing radiations. Dr Zhadobov was the recipient of the 2005 Best Poster Presentation Award from the International School of Bioelectromagnetics, 2006 Best Scientific Paper Award from the Bioelectromagnetics Society, and Brittany's Young Scientist Award in 2010.

Nacer Chahat was born in Angers, France, in 1986. He graduated in electrical engineering and radio communications from the Ecole Supérieur d'ingénieurs de Rennes (ESIR) and received the Master's Degree in Telecommunication and Electronics in 2009. Since 2009, he has been working toward the Ph.D. degree in signal processing and telecommunications at the Institute of Electronics and Telecommunications of Rennes (IETR), University of Rennes 1, Rennes, France. His current research fields are millimeter-wave antennas, and the evaluation of the interaction between the electromagnetic field and human body. He accomplished a 6-month master's training period as a special research student in 2009 at the Graduate School of Engineering, Chiba University, Chiba, Japan. Mr Chahat was the recipient of the 2011 Best Poster Presentation Award from the Bioelectromagnetics Society.

Ronan Sauleau graduated in 1995 from the "INSA de Rennes", Rennes, France. He joined the "Ecole Normale Supérieure de Cachan" in 1995 and received the "Agrégation" in 1996. He received the Ph.D. degree from the University of Rennes 1 in 1999. He received the "Habilitation à Diriger des Recherches" in November 2005 and is Full Professor since November 2009. His current research fields are numerical modeling (mainly FDTD), millimeter-wave

https://doi.org/10.1017/S1759078711001000 Published online by Cambridge University Press

printed and reconfigurable (MEMS) antennas, lens-based focusing devices, periodic and non-periodic structures (electromagnetic bandgap materials, metamaterials, reflectarrays, and transmitarrays) and biological effects of millimeter waves. He holds 5 patents and has co-authored more than 100 journal papers and 240 publications in national and international conferences. He received the 2004 ISAP Young Researcher Scientist Fellowship (Japan) and the first Young Researcher Prize in Brittany, France in 2001. In 2007, he was elevated as a Junior Member of the "Institut Universitaire de France". He received the Bronze Medal from CNRS in 2008.

https://doi.org/10.1017/S1759078711001000 Published online by Cambridge University Press